C. R. Chimie 22 (2019) 161–168

Contents lists available at ScienceDirect

Comptes Rendus Chimie

www.sciencedirect.com

Full paper/Mémoire

External mass transport process during the adsorption of fluoride from aqueous solution by activated clay

Processus de transport de matière externe au cours de l'adsorption d'ions fluorure sur une argile activée

Sami Guiza*, Houda Hajji, Mohamed Bagane

Department of Chemical Engineering Process, National Engineering School of Gabés, University of Gabés, Street Omar Ibn El Khattab, 6029 Gabés, Tunisia

ARTICLE INFO

Article history:
Received 13 October 2018
Accepted 4 February 2019
Available online 6 March 2019

Keywords:
Adsorption
Modified clay
Fluoride removal
Kinetics
External mass transport

ABSTRACT

The removal of fluoride ions from an aqueous solution using a modified sulfuric acid clay was studied in batch adsorption. The adsorption kinetics were studied to identify the retention mechanisms. For kinetics study, perfectly stirred batch experiments were carried out after the adjustment of the parameters influencing the system, such as the pH, the adsorbent dosage, the initial concentration of fluoride ions, and the stirring speed. It appears that the rate of fluoride ion removal (1) increased with the mass of adsorbent and the stirring speed, and (2) decreased with the initial fluoride ion concentration. The experimental results were adjusted according to kinetic equations representing four external transport models. The latter were used to calculate the external mass transfer coefficient, k_f. The results showed that this coefficient is in the range of 10^{-5}–10^{-4} m s^{-1}.

Mots clés:
Adsorption
Argile modifiée
Élimination des ions fluorure
Cinétique
Transfert de masse externe

RÉSUMÉ

Nous avons étudié dans ce travail la cinétique d'adsorption en solution aqueuse des ions fluorure sur un matériau argileux modifié par l'acide sulfurique dans un adsorbeur en batch. L'influence de certains paramètres, comme le pH de la solution, la masse d'argile en solution, la concentration initiale des ions fluorure et la vitesse d'agitation, a été étudiée. Les résultats obtenus prouvent que : (i) la cinétique augmente avec la masse d'argile et la vitesse d'agitation et (ii) décroît avec la concentration initiale en ions fluorure. Quatre modèles de transport externe ont été étudiés et ont montré que l'ordre de grandeur du coefficient k_f se trouve dans la gamme entre 10^{-5} et 10^{-4} m s^{-1}.

1. Introduction

Water pollution is recognized as one of the major problems in the world. It represents a serious threat to human health because of the uncontrolled industrial discharges, the intensive use of chemical fertilizers in

* Corresponding author.
E-mail address: sami_guiza@yahoo.fr (S. Guiza).

https://doi.org/10.1016/j.crci.2019.02.001
1631-0748/

agriculture, and the disorderly exploitation of water resources. Many minerals such as Ca^{2+}, Mg^{2+}, Na^{+}, Cl^{-}, and F^{-} are essential to the body; however, the excessive intake of these substances can cause harmful effects to human health and the environment [1]. In addition to arsenic and nitrate, fluoride ions (F^{-}) have been classified as one of the most dangerous groundwater contaminants that lead to large-scale health problems by the World Health Organization [2]. Different technologies such as adsorption [3,4], oxidation [5], ion exchange [6], precipitation [7], electrodialysis [6], and reverse osmosis have been used for fluoride removal from water. Adsorption is reported as one of the most effective and economical techniques for water defluorination. The adsorption process is known to be simple and efficient in pollutant treatment in concentrated form at a low cost. In addition, it is relatively considered as an environmentally friendly process [7]. Many low-cost adsorbents have been used for fluoride removal from water [8,9], including activated alumina [10], activated carbon [11], kaolinite, bentonite, and montmorillonite [12], and so forth. The frequent use of clays is mainly because of their abundance and large reactive surface. In addition, clays can be preferred to synthetic adsorbent materials because of their relatively low costs [13].

Clay and clay mineral application in fluoride removal from water is well supported in the literature. In fact, considerable quantities of montmorillonite, kaolinite, or pyrophyllite clay display a huge potential for fluoride adsorption [14–16]. The positively charged surface of clay minerals provides an explanation for the high affinity uptake of the negatively charged ions at near neutral pH. The fluoride removal capacity of clay and clay minerals is impacted by different factors, such as pH and the medium's strength, and thermodynamic conditions [17,18]. Raw clay and clay minerals are rarely used and they are often used after physicochemical modifications such as metal oxide amendment, acid treatment, and thermal activation. Such modifications enhance stability at the optimal operating pH, active sites accessibility, adsorption capacity, and surface area [17,19]. Effective defluoridation with acid-activated kaolinite compared with raw kaolinite, where maximum sorption capacity of acid-activated clay ranged between 0.0450 and 0.0557 mg g^{-1} at different temperatures, was reported in Ref. [20].

In the past decades, most articles on fluoride adsorption onto clay fields have interpreted the results with a pseudo-first-order or pseudo-second-order kinetic models [14,17,19,21,22]. Besides, Elovich kinetics model has been applied to chemisorption on the heterogeneous surface [4]. The traditional and routine fitting with pseudo-first-order and pseudo-second-order kinetic equations can sometimes give good fits with a coefficient of determination or correlation function (R^2) values greater than 0.995 as this is the case here. However, we cannot be assured of an equation that does not give a correct time variation in the rate and veils the true evolution of the kinetics, whose rate is not necessarily uniform (pseudo-first-order), linear (pseudo-second-order). Nevertheless, it is well documented in the literature that the overall adsorption in a porous adsorbent must not only consider the adsorption rate on an active site but also the external mass transfer, surface diffusion, intraparticle diffusion, and pore volume diffusion [21].

The aims of this work were as follows: first, to study the fluoride adsorption kinetics onto activated clay; second, to assess the solution agitation speed, initial fluoride ion concentration, and adsorbent dosage effect on matter transfer rate, and eventually to find a simple mathematical model suitable for a better understanding of the physical phenomena involved in a more appropriate design, operation, optimization, and control of the industrial process separation. Simplified models of external diffusion are tested to describe the adsorption process. The external diffusion coefficient, k_f, is determined using different models and then correlated with the experimental variables.

2. Experimental section

2.1. Materials

In this work, bentonite clay selected from an El-Hicha site in the south of Tunisia was used as a raw material. The material was purified by aqueous dispersion and decantation. After the purification process, the clay remained quartz free and the fraction with a particle size less than 40 μm was separated and subjected to activation. Sulfuric acid treatments were used to increase the clay mineral surface area and to obtain high porosity.

The activated sample was obtained according to the following procedure: 100 g of material clay micropowder was mixed with an aqueous H_2SO_4 solution (acid concentration of 13.8%) in a jacketed glass reactor regulated at a fixed temperature (75 °C) by a thermostated bath for 3.75 h under mechanical stirring at 200 rpm. Then, it was washed with distilled water many times until pH of 6 was reached. The obtained samples were dried at 60 °C for 24 h.

The physicochemical and textural characteristics using the Brunauer, Emmett and Teller method (BET), described in a previous work [24] are shown in Table 1.

2.2. Adsorption test experiments

A sodium fluoride stock solution was prepared by dissolving 2.21 g of sodium fluoride (analytic reagent grade) in 1000 mL of double glass distilled water, the stock solution

Table 1
Physicochemical properties of the studied clay samples.

Chemical composition (% by weight)	Natural clay	Acid activated clay
SiO_2	47.70	50.12
Al_2O_3	18.71	18.26
Fe_2O_3	12.37	9.12
CaO	3.67	1.93
MgO	2.59	1.89
K_2O	1.05	0.87
Na_2O	0.96	0.17
P_2O_5	0.32	0.02
SO_3	0.96	4.91
Li	14	12
Structural parameters		
Specific surface of BET (m^2 g^{-1})	86	167
Total pore volume (cm^3 g^{-1})	0.1394	0.1986
Mean pore diameter (Å)	40.53	49.03

of desired fluoride concentration. The residual fluoride concentration in each sample was determined using ion selective electrode, fluoride electrode, and "Orion ion analyzer" model 9409-SC.

2.3. Equilibrium isotherm studies

To determine the activated clay adsorption capacity of the fluoride ion, 1 g of activated clay was added into 100 mL of fluoride ion solutions with initial concentrations ranging between 50 and 500 mg L^{-1}. The resulting suspensions were shaken at a constant stirring rate 400 rpm for 3 h to reach equilibrium. The experiments were carried out at 25 °C with a pH value adjusted to 5 [25].

The amount of fluoride adsorbed onto the activated clay at equilibrium, q_e (mg g^{-1}), was obtained as follows:

$$q_e = \frac{(C_0 - C_e)V}{m} \quad (1)$$

where C_0 and C_e are the initial and equilibrium fluoride ion concentrations in solution, respectively, and m is the mass of dry activated clay (g).

2.4. Batch kinetic studies

The study is carried out at the laboratory in a liquid phase in an agitated "adsorber" tank operating in batch mode. It is a 2 L volume jacketed reactor maintained at constant temperature and equipped with a paddle stirrer. We introduced 1 L of fluoride ion solution at concentrations ranging from 30 to 90 mg L^{-1}, for different mass adsorbents varying from 0.5 to 1.5 g and different stirring speeds ranging between 150 and 300 rpm and at pH 5 and at a temperature of 25 °C. The samples taken intermittently made it possible to pursue the concentration of fluoride solution residual. Samples of 5 mL were taken and centrifuged for a minimum time at a speed of 2000 rpm [26]. The fluoride solution residual concentration was determined from a previous calibration curve. We follow for a dry activated clay mass of 1 g L^{-1} of solution, an initial fluoride ion concentration of 30 mg L^{-1}, a variable stirring speed, and the evolution of the reduced concentration, C_t/C_0, with function of time.

3. Theoretical model

The solute adsorption mechanism on the surface of a solid goes through several successive elementary stages. Each of these stages can control the global phenomenon under given conditions. Fluoride adsorption requires (1) sorbate transport from the bulk of the solution to the exterior film surrounding the adsorbent; (2) sorbate movement across the external liquid film boundary layer to external surface sites; and (3) sorption of sorbate at internal surface sites. The last step is much faster than the first two and consequently its contribution to the overall resistance to the adsorption process is often neglected. Accordingly, the limiting step of the process can be of external type, internal type, or both.

Two resistance models are very complex because the transfer equations are coupled and the resolution of the equation system requires numerical resolution methods.

It is difficult to predict if one or both resistances (external or internal) limit the overall process without adsorption experiments.

Several researchers have studied the problem of external transport to define the conditions under which the hypotheses of this type of transfer and consequently the calculating method of the coefficient in the outer film, k_f, are valid [23,27]. In all these calculating methods k_f the resistance in the outer film is the limiting step at the beginning of adsorption.

In the present work, we faced the problem of determining the method of choice for calculating k_f and so retain the model that best describes the physical reality of the adsorption process. Therefore, four methods taken from the bibliography, namely, the following models of the initial slopes of Furusawa and Smith (Model I), Mathews and Weber (Model II) [23], Furusawa and Smith for a linear isotherm (Model III), and dimensional analysis of Harriott (Model IV) [23] were tested. Note that the first three methods are based on experimental adsorption data whereas the last is completely empirical.

3.1. Model of initial slopes

This model was initially used in the adsorption of benzene on activated carbon [27]. In a perfectly stirred adsorber, the solute concentration, C_t, at different times and the solid concentration, m_s, were supposed to be uniform within the liquid phase. m_s can be calculated by the following equation:

$$m_s = \frac{m}{V} \quad (\text{g L}^{-1}) \quad (2)$$

where m and V denote the solid mass and the liquid phase volume treated in the adsorber, respectively.

For average diameter spherical particles, d_p, bulk density, ρ_p, and external exchange area can be obtained as follows:

$$A_p = \frac{6m_s}{d_p\rho_p} \quad (\text{m}^{-1}) \quad (3)$$

The solute concentration variation in the liquid phase as a function of time is related to the external transfer coefficient, k_f (m s^{-1}), by the following relation:

$$\frac{dC_t}{dt} = -k_f A_p (C_t - C_s) \quad (\text{mg L}^{-1}\ \text{s}^{-1}) \quad (4)$$

where C_s is the liquid phase solute concentration at the outer surface of the particles. At the beginning of the adsorption process, the concentrations C_s and C_t tend to 0 and C_0, respectively, and consequently neglecting the internal diffusion of the solute. Eq. 3 then becomes

$$\left[\frac{dC_t/C_0}{dt}\right]_{t=0} = -k_f A_p \quad (\text{s}^{-1}) \quad (5)$$

Thus k_f can simply be determined from the initial slope of the curve C_t/C_0 as a function of time. Then, the values of k_f are correlated with each variable (concentration, stirring speed, and adsorbent dosage), X, by a general equation of the type [23]

$$k_f = B\,X^p \quad (\mathrm{m\,s^{-1}}) \tag{6}$$

where B and p are two constants to be determined from the experimental data.

3.2. Model of Mathews and Weber

The integration of Eq. 4, when t and C_s tend to zero, leads to

$$\ln\frac{C_t}{C_0} = -k_f A_p t \tag{7}$$

Under these conditions k_f can be calculated rapidly from the slope of the line $\ln(C_t/C_0)$ as a function of time t.

3.3. Linear model of Furusawa and Smith (FS)

In the case where the equilibrium between the solute and the solid is of the linear type ($q_e = K_L C_e$), the equation of the model will be [28]

$$\ln\left(\frac{C_t}{C_0} - \frac{1}{1+m_s K_L}\right) = \ln\left(\frac{m_s K_L}{1+m_s K_L}\right) - \left[\left(\frac{1+m_s K_L}{m_s K_L}\right) k_f A_p t\right] \tag{8}$$

From the ordinate at the origin, $m_s K_L/(1 + m_s K_L)$, and the slope, $-((1 + m_s K_L)/m_s K_L) k_f A_p$, of the line $\ln(C_t/C_0 - 1/(1 + m_s + K_L))$ as a function of time, k_f is deduced.

3.4. Dimensional analysis: Harriot method

According to Harriot, the material transfer coefficient between the liquid and the suspended particles in a stirred tank, k_f, can be calculated from the Tien relation [28]:

$$\frac{k_f}{k_f^*} \cong 2 \tag{9}$$

where k_f^* is the material transfer coefficient of particles moving at their terminal velocities, u_t (m s^{-1}), within the liquid. To estimate k_{f^*}, Harriot suggests the use of the Ranz–Marshall correlation [29]:

$$\frac{k_f^* d_p}{D_m} = 2 + 0.6\left(\rho\frac{d_p u_t}{\mu}\right)^{0.5}\left(\frac{\nu}{D_m}\right)^{0.33} \tag{10}$$

The molecular diffusion coefficient of the solute in the liquid phase, D_m, is given by the Wilke–Chang relation [30]:

$$D_m = \frac{(117.3\ 10^{-18})(\varphi M)^{0.5} T}{\mu V_m^{0.6}} \quad (\mathrm{m^2 \cdot s^{-1}}) \tag{11}$$

where φ is the solvent–fluoride ion association factor (for water $\varphi = 2.26$) [31].

4. Results and discussion

4.1. Equilibrium studies

The equilibrium biosorption data are analyzed using the Langmuir model as shown by the following equation:

$$q_e = \frac{q_m b C_e}{1 + bC_e} \tag{12}$$

where q_e is the biosorption capacity at equilibrium (mg g^{-1}), C_e is the fluoride ion concentration at equilibrium (mg L^{-1}), and q_m (mg g^{-1}) and b (L g^{-1}) are the Langmuir's constants. The essential characteristics of Langmuir isotherm can be expressed in terms of a dimensionless constant separation factor or equilibrium parameter R_L, which is defined by Weber [26].

$$R_L = \frac{1}{(1 + K_L\ C_0)} \tag{13}$$

Fig. 1 shows the Langmuir isotherm plots of the experimental data for fluoride ion biosorption onto activated clay. The isotherm constants of the Langmuir model are shown in Table 2. The results indicate that the adsorption capacity of activated clay particles is high for the F^- 75.757 mg g^{-1} at 25 °C. The R_L values dictate favorable adsorption for $0 < R_L < 1$. On the basis of the $R^2 = 0.995$, there is an overall agreement that Langmuir model is the most suitable for designing industrial adsorption processes. The comparison of maximum adsorption capacity of F^- ions onto various adsorbents is presented in Table 3. It

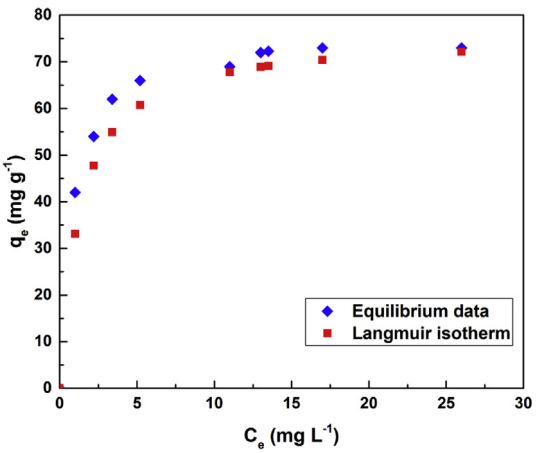

Fig. 1. Adsorption of fluoride ions onto activated clay using the Langmuir isotherm.

Table 2
Langmuir isotherm constants for fluoride ions onto activated clay.

Constants	q_m (mg g^{-1})	b (L mg^{-1})	$K_L = b \times q_m$ (L g^{-1})	R_L	R^2
Fluoride	75.757	0.776	58.787	0.36	0.995

shows that the activated clay studied in this work has acceptable adsorption capacity.

4.2. Kinetic studies – external mass transfer

4.2.1. Stirring speed effect

Fig. 2 shows that adsorption rate depends on the stirring speed, N, and that it is fast for $t < 20$ min, then it slows down. This phenomenon can be due to the increase in the stirring speed, which affects the resistance to the material transfer outside the clay particle [34]. Hereafter, for the calculation of k_f, we will detail the method of initial slopes for its simplicity. Fig. 3 shows the variation of ln k_f as a function of ln N. Relying on this variation, we found the following correlation between k_f and N: $k_f = 1.077 \times 10^{-4} N^{0.639}$

4.2.2. Adsorbent dosage effect

Fig. 4 illustrates that for a contact time of 20 min, the adsorption kinetics goes up by increasing the mass of clay to 1.5 g. It also displays beyond 90 min, the material transfer rate tends to zero. As shown in Fig. 5, the correlation between k_f and m is

$$k_f = 22.965 \times 10^{-4} m^{0.55}$$

This result indicates that the fluoride solute transport in the outer film is also controlled by the clay mass in solution. Increasing the mass of clay in solution helps to augment the liquid film transfer coefficient. Literature in general indicates an increased removal efficiency (RE) with adsorbent dose. Kim et al. [35] observed that an increase in pyrophyllite dose (from 0.05 to 2.0 L^{-1}) improves the RE (25–98.5%) at a fixed initial fluoride concentration. Similar observations have been reported by others [19,36] while carrying out fluoride removal studies with kaolinite and bentonite. It can be inferred from the literature that the increase in RE is mainly attributed to the enhancement number of active sites available for adsorption of fluoride ions.

Table 3
Clay minerals used for fluoride removal from water.

Clay mineral	Adsorption capacity (mg g^{-1})	Applied isotherm model	Reference
Magnesium incorporated bentonite	2.26	Langmuir	[19]
Fe^{3+} modified bentonite	2.91	Langmuir	[17]
Montmorillonite	1.32	Langmuir	[14]
Pyrophyllite	2.2	Langmuir	[15]

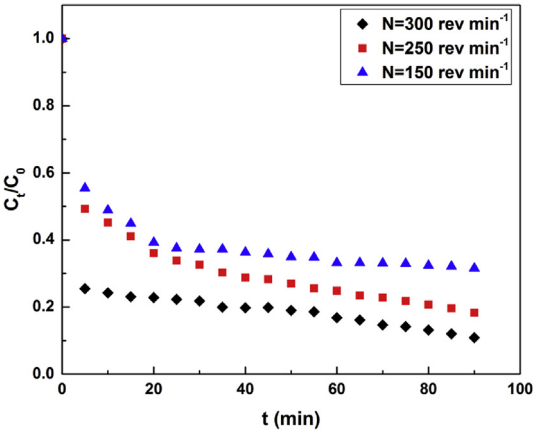

Fig. 2. Effect of the stirring speed (pH = 5, T = 25 °C, m = 1 g, C_0 = 30 mg L^{-1}).

4.2.3. Initial concentration effect

Fig. 6 shows that the adsorption is faster at its beginning than at its end. For instance, after 40 min, the adsorption slows down: this deceleration is probably because of the

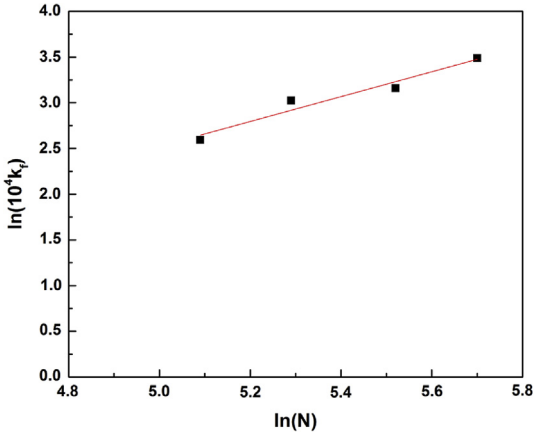

Fig. 3. ln(10^4 k_f) versus ln(N).

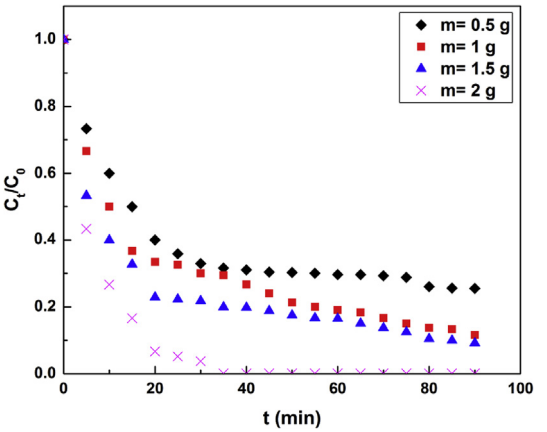

Fig. 4. Adsorbent dosage effect (pH = 5, T = 25 °C, C_0 = 30 mg L^{-1}, N = 250 rpm).

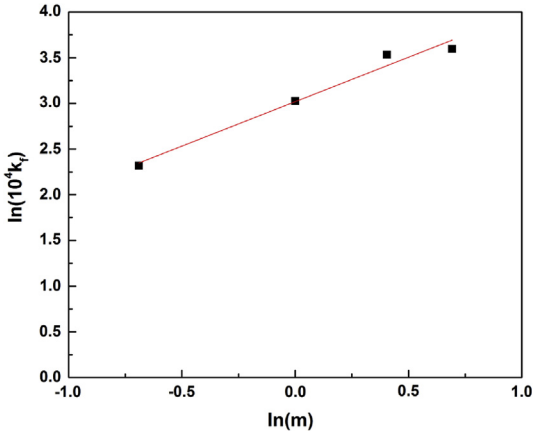

Fig. 5. $\ln(10^4\ k_f)$ versus $\ln(m)$.

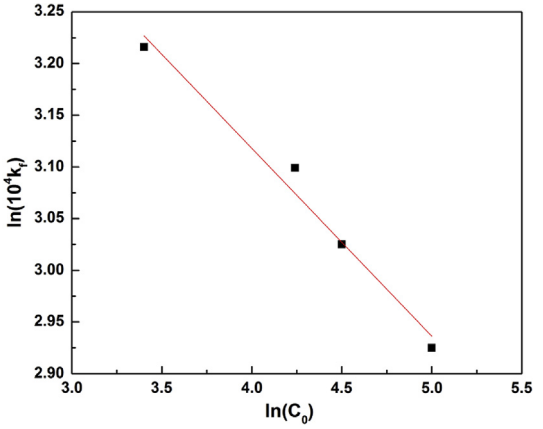

Fig. 7. $\ln(10^4\ k_f)$ versus $\ln(C_0)$.

resistance to the material transfer inside clay particles. Toward high concentrations, the gap becomes tight and the adsorbed fraction is small. In addition, the time required to reach equilibrium varies with the initial fluoride concentration. As shown in Fig. 7, the correlation between k_f and C_0 is

$$k_f = 36.52 \times 10^{-4} C_0^{-0.132}$$

The negative value of p indicates that, for the fluoride/clay pair studied, the transfer coefficient in the outer film decreases with the initial fluoride ion concentration, in agreement with the observations of Mckay et al. [37]. Using magnesium incorporated bentonite and pyrophyllite [15,19] showed that increase in initial fluoride concentration leads to a decrease in RE. The authors explained the behavior in terms of exhausted binding capacity of bentonite or increased competition for the active adsorption sites at higher fluoride concentration.

Table 4 regroups the final and complete result of k_f values calculated by the different models. Table 5 involves a comparison between our results and those found in the bibliography. Thus, we remark the following:

- Despite the diversity of studied pairs, the magnitude order of k_f is in the range of 10^{-5}–10^{-4} m s^{-1}.
- For all solute/adsorbent pairs, an increase in variation of k_f with m.
- The effect of the initial solute concentration is negative: an effect contrary to that of the stirring speed.
- The calculation of k_f by the adimensional analysis method does not provide the variation of this coefficient with the initial concentration and the mass of adsorbent in solution. Besides, the laws of the boundary layer theory state that k_f is proportional to the solute diffusion coefficient of the solute in the surrounding medium and the flow conditions around the solid particles. We made this variation with C_0 and m at the concentration gradient established at the beginning of the adsorption process. Despite this handicap by this method, the order of magnitude of k_f is always in the margin mentioned.
- The difference between the values of k_f calculated by models II and III is very small. This result is attributed to the term $m_s \times K_L/(1 + m_s \times K_L)$, which is almost equal to 1 in the case of the study couple. The use of Model I for the experimental determination of k_f can be suggested because of its simplicity.

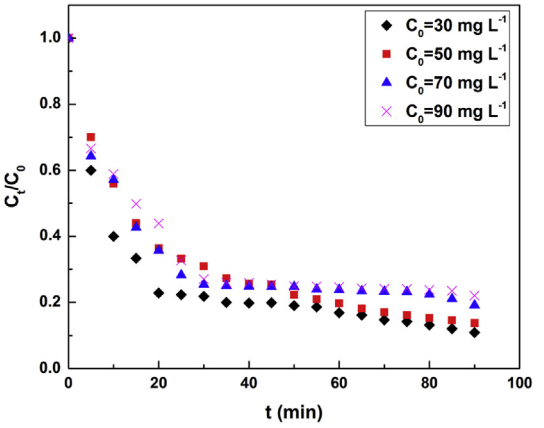

Fig. 6. Effect of the initial concentration (pH = 5, T = 25 °C, m = 1 g, N = 250 rpm).

Table 4
Results of the calculation of k_f by the different models ($\times 10^{-5}$ m s^{-1}).

Solute	Effect of model		I	II	III	IV
F^-	N (rpm)	150	13.38	1.86	1.68	13.5
		200	20.60	2.17	1.89	20.3
		250	23.62	2.27	1.95	23.5
		300	33.07	2.47	2.70	33.45
	C_0 (mg L^{-1})	10	10.89	3.10	2.52	33.45
		30	10.23	2.49	2.00	33.45
		50	8.00	2.10	1.19	33.45
		70	7.66	1.50	1.65	33.45
	m (g)	0.5	10.23	1.44	1.65	33.45
		1	20.60	2.75	2.57	33.45
		1.5	34.25	3.75	4.44	33.45
		2	36.48	7.08	9.52	33.45

Table 5
External transfer coefficient k_f (m s^{-1}); comparison with the bibliography.

Adsorbent	Field of validity	Solute	Variables			Model	Reference
			N (rpm)	C_0 (g L^{-1}) or T (°C)	m (g)		
Bone char	$2 \le C_0 \le 5$ mmol/L $6.5 \le m \le 10.5$ g $250 \le d_p \le 100$ µm	Cd^{2+} Cu^{2+} Zn^{2+}		$4.36 \times 10^{-6} \le k_f \le 7.30 \times 10^{-6}$ $6.14 \times 10^{-4} \le k_f \le 1.0 \times 10^{-3}$ $4.75 \times 10^{-4} \le k_f \le 7.39 \times 10^{-4}$	$5.47 \times 10^{-6} \le k_f \le 6.23 \times 10^{-6}$ $8.01 \times 10^{-6} \le k_f \le 8.99 \times 10^{-6}$ $5.34 \times 10^{-6} \le k_f \le 6.40 \times 10^{-6}$	FS	[23]
Natural clay	$207 \le N \le 684$ rpm $0.05 \le m \le 0.25$ g $5 \le C_0 \le 30$ mg L^{-1} $0.45 \le d_p \le 1.75$	BM VM RC	$k_f = 2.73 \times 10^{-5} N^{0.28}$ $k_f = 1.22 \times 10^{-5} N^{0.19}$ $k_f = 1.26 \times 10^{-9} N^{1.81}$	$k_f = 5440 \times 10^{-5} C_0^{-1.91}$ $k_f = 11.63 \times 10^{-5} C_0^{1.4}$ $k_f = 17.1 \times 10^{-5} C_0^{0.66}$	$k_f = 190 \times 10^{-5} m^{1.83}$ $k_f = 7.57 \times 10^{-5} m^{0.28}$ $k_f = 26 \times 10^{-5} m^{0.88}$	FS	[32]
China clay	$30 < T < 50$ °C	F^-		$2.716 < k_f < 5.042 \times 10^{-5}$		FS	[33]
Activated clay	$150 \le N \le 300$ rpm $0.5 \le m \le 1.5$ g $30 \le C_0 \le 90$ mg L^{-1}	F^-	$k_f = 1.077 \times 10^{-4} N^{0.639}$	$k_f = 36.52 \times 10^{-4} C_0^{-0.132}$	$k_f = 22.965 \times 10^{-4} m^{0.55}$	FS	This study

5. Conclusions

In the present work, we studied the adsorption kinetics of fluoride onto activated clay to design an industrial adsorber. It was demonstrated in the first part that the optimal adsorption time is 30 min for a solution clay concentration of 1.5 g L^{-1}, at a minimum stirring speed of 300 rpm. Under these conditions, the pollutant elimination rate is greater than 90%. The transfer coefficient in the outer boundary layer was determined. This coefficient varied with the agitation speed, the initial fluoride ion concentration, and the adsorbent mass. Despite the diversity of the studied pairs, k_f magnitude order was in the range of 10^{-5}–10^{-4} m s^{-1}.

Nomenclature

A_P surface area of sorbent (m^{-1})
B equation constant
b Langmuir isotherm constant (g L^{-1})
C_r liquid phase concentration at radius r (mg L^{-1})
C_0 initial liquid phase concentration (mg L^{-1})
C_e equilibrium liquid phase concentration (mg L^{-1})
C_s liquid phase concentration at external sorbent surface (mg L^{-1})
C_t liquid phase concentration at time t (mg L^{-1})
D_m molecular diffusion coefficient of fluoride ions (m^2 s^{-1})
d_p: diameter of sorbent (m)
K_L: Langmuir constant (L g^{-1})
k_f External mass transfer coefficient (m s^{-1})
k_{f^*} Equilibrium external mass transfer coefficient (m s^{-1})
m mass of dry sorbent (g)
M molecular weight of the solvent (g mol^{-1})
m_s concentration of sorbent (g L^{-1})
N stirring speed (rpm)
P equation constant
r radius of concentration front of metal ions penetrating adsorbent (m)
t contact time (s)
u_t terminal velocity (m s^{-1})
V liquid phase volume (L)
V_m molar volume (m^3 mol^{-1})
φ solvent-fluoride ion association factor (pour l'eau $\varphi = 2.26$)
μ dynamic viscosity of fluid (kg m^{-1} s^{-1})
ν kinematic viscosity (m^2 s^{-1})
ρ_p: particle density (kg m^{-3})
ρ solution density (kg m^{-3})

References

[1] N.A. Oladoja, B. Helmreich, Chem. Eng. J. 258 (2014) 51–61.
[2] S. Ravulapalli, R. Kunta, J. Fluorine Chem. 193 (2017) 58–66.
[3] A. Vinati, B. Mahnty, S.K. Behera, Appl. Clay Sci. 114 (2015) 340–348.
[4] M.G. Sujana, S. Anand, Desalination 267 (2014) 222–227.
[5] A.P. Viacheslav, M. Will, J. Fluorine Chem. 169 (2015) 6–11.
[6] V. Khatibikamal, A. Torabian, F. Janpoor, G. Hoshyaripour, J. Hazard. Mater. 179 (2010) 276–280.
[7] A. Bhatnagar, E. Kumar, M. Sillanpaa, Chem. Eng. J. 171 (2011) 811–840.
[8] K. Singh, D. H Lataye, K.L. Wasewar, J. Fluorine Chem. 194 (2017) 23–32.
[9] L. Vinnett, M. Alvarez-Silva, A. Jaques, F. Hinojosa, J. Yianatos, Miner. Eng. 77 (2015) 167–171.
[10] N. Sakhare, S. Lunge, S. Rayalu, S. Bakardjiava, J. Subrt, S. Devotta, N. Labhsetwar, Chem. Eng. J. 203 (2012) 406–414.
[11] A.K. Yadav, R. Abbasi, A. Gupta, M. Dadashzadech, Ecol. Eng. 52 (2013) 211–218.
[12] B. Kemer, D. Ozdes, A. Gundogdu, V.N. Bulut, C. Duran, M. Soylak, J. Hazard. Mater. 168 (2009) 888–894.
[13] S. Guiza, M. Bagane, J. Univ. Chem. Technol. Metall. 14 (2012) 283–288.
[14] A. Ramdani, S. Taleb, A. Benghalem, N. Ghaffour, Desalination 250 (2009) 408–413.
[15] A. Goswami, M.K. Purkait, Separ. Sci. Technol. 46 (2011) 1797–1807.
[16] V. Tomar, Desalination 201 (2006) 267–276.
[17] W.M. Gitari, T. Ngulube, V. Masindi, J.R. Gumbo, Desalin. Water Treat. 53 (2013) 1578–1590.
[18] R. Srinivasan, Adv. Mater.Sci. Eng. (2011) 1–17.
[19] D. Thakre, S. Rayalu, R. Kawade, S. Meshram, J. Subrt, N. Labhsetwar, J. Hazard. Mater. 180 (2010) 122–130.
[20] P.K. Gogoi, R. Baruah, J. Chem. Technol. 15 (2008) 500–503.
[21] M. Mobarek, A.Q. Selim, E.A. Mohamed, M.K. Seliem, J. Clean. Prod. 192 (2018) 712–721.
[22] A. Maiti, J.K. Basu, S. De, Desalination 265 (2011) 28–36.
[23] K.H. Choy Keith, C.K.K. Danny, C.W. Chun, J.F. Porter, M.K. Gordon, J. Colloid Interface Sci. 271 (2004) 284–295.

[24] S. Guiza, M. Bagane, A. Al-Soudani, H.A. Amor, Adsorpt. Sci. Technol.. 22 (2004) 245–255.
[25] S. Guiza, L. Frank, M. Bagané, Desalin. Water Treat. 113 (2018) 262–269.
[26] S. Guiza, Ecol. Eng. 99 (2017) 134–140.
[27] T. Furusawa, J.S. Smith, Ind. Eng. Chem. Fundam. 12 (1973) 197–202.
[28] C. Tien, Adsorption Calculations and Modelling, Butterworth-Heinemann, Newton, MA, USA, 1994.
[29] W.E. Ranz, W.R. Marshall, Chem. Eng. 48 (1952) 141–146.
[30] T. Furusawa, J.S. Smith, AIChE J. 19 (1973) 401–405.
[31] R.E. Treybal, Mass Transfer-Operations, 3rd ed., Mc Graw-Hill, New York, 1981.
[32] S. Guiza, M. Bagane, J. Water Sci. 26 (2013) 39–51.
[33] A.K. Chaturvedi, K.C. Pathak, V.N. Singh, Appl. Clay Sci. 3 (1988) 337–346.
[34] C.J. Geankoplis, Transport Processes and Separation. Processes Principles, Prentice Hall, USA, 2003.
[35] J.H. Kim, C.Q. Lee, J.A. park, J.K. Kang, N.C. Choi, S.b. Kim, Desalin. Water Treat. 51 (2012) 3408–3416.
[36] S. Meenaskshi, C.S. Sundaram, R. Sukumar, J. Hazard. Mater. 153 (2008) 164–172.
[37] G. Mckay, M. El Geund, M.M. Nassar, Trans IChemE 74 (1996) 277–288.